

Activation of a Bacterial Mechanosensitive Channel in Mammalian Cells by Cytoskeletal Stress

JOHANNA HEUREAUX,¹ DI CHEN,² VICTORIA L. MURRAY,¹ CHERI X. DENG,² and ALLEN P. LIU^{1,2,3,4}

¹Department of Mechanical Engineering, University of Michigan, 2350 Hayward Street, Ann Arbor, MI 48105, USA;

²Department of Biomedical Engineering, University of Michigan, Ann Arbor, MI, USA; ³Cellular and Molecular Biology Program, University of Michigan, Ann Arbor, MI, USA; and ⁴Biophysics Program, University of Michigan, Ann Arbor, MI, USA

(Received 29 January 2014; accepted 20 May 2014; published online 3 June 2014)

Associate Editor Cynthia A. Reinhart-King oversaw the review of this article.

Abstract—Cells can sense a myriad of mechanical stimuli. Mechanosensitive channel of large conductance (MscL) found in bacteria is a well-characterized mechanosensitive channel that rapidly responds to an increase in turgor pressure. Functional expression of MscL in mammalian cells has recently been demonstrated, revealing that molecular delivery or transport can be achieved by charge-induced activation of MscL. Despite a well-accepted mechanism for MscL activation by membrane tension in bacteria, it is not clear whether and how MscL can be opened by other modes of force transduction in mammalian cells. In this work, we used a variety of techniques to characterize the gating of MscL expressed in mammalian cells, using both wild type and a G22S mutant which activates at a lower threshold. In particular, employing a recently developed technique, acoustic tweezing cytometry (ATC), we show that ultrasound actuation of integrin-bound microbubbles can lead to MscL opening and that ATC induced MscL activation was depen-

dent on the functional linkage of the microbubbles with an intact actin cytoskeleton. Our results indicate that localized mechanical stress can mediate opening of MscL that requires force transduction through the actin cytoskeleton, revealing a new mode of MscL activation that may prove to be a useful tool for mechanobiology and drug delivery research.

Keywords—Mechanosensitive channels, Mechanobiology, Acoustic tweezing cytometry, Membrane tension.

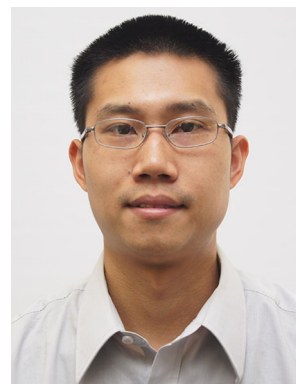
INTRODUCTION

A key challenge in mechanobiology is to understand how mechanical signals interact with biochemical signaling pathways. It is known that mechanical and biochemical signaling networks are coupled through proteins that undergo large conformational changes, and a number of mechanisms have been shown to mediate the mechanochemical signal conversion.³⁷ For example, stretching of mechanosensitive (MS) proteins can damage molecular binding sites, expose regulatory sites, or alter association/dissociation rates for protein binding.^{6,15,18} Mediated by membrane stretching, MS

Address correspondence to Allen P. Liu, Department of Mechanical Engineering, University of Michigan, 2350 Hayward Street, Ann Arbor, MI 48105, USA. Electronic mail: allenliu@umich.edu

This paper is part of the 2014 Young Innovators Issue.

Allen P. Liu received a B.Sc. degree in Biochemistry (Honours) from the University of British Columbia, Vancouver, Canada, in 2001. He obtained his Ph.D. in Biophysics in 2007 from the University of California-Berkeley, receiving two fellowships from the Natural Sciences and Engineering Research Council of Canada. As a graduate student in Daniel Fletcher's lab, he studied the dynamic interplay between actin networks and membrane using a reconstituted system. From 2007 to 2011, he was a post-doctoral fellow in Sandra Schmid and Gaudenz Danuser's labs in the Department of Cell Biology at The Scripps Research Institute in La Jolla, CA, while holding a post-doctoral fellowship from the Leukemia and Lymphoma Society. By combining live cell total internal reflection fluorescence microscopy and high-content image analysis, he studied the role of cortical tension and clustering of cargo molecules in regulating the dynamics of clathrin-coated pits. Since January 2012, he has been an Assistant Professor in the Department of Mechanical Engineering and Biomedical Engineering at the University of Michigan. He is a recipient of the NIH Director's New Innovator Award. His current research interests include cell mechanics, mechanobiology, and synthetic biology.



channel opening can lead to direct ion influx.²³ MS channels are central to mechanosensory transduction and essential for a variety of physiological processes, including regulation of cell shape and volume, and sensing touch and sound.^{2,23}

MS channels possibly originated very early during the evolution of living organisms because primordial microbes needed to cope with osmotic forces due to the constant changes of osmolarity in their environments. Indeed, the prototypical MS channels in bacteria serve as emergency release valves that allow cytoplasmic solutes to be rapidly released from the cells. Most microbes possess members of one or both families of the MS channels, mechanosensitive channels of small conductance (MscS) and MscL. The best studied of these MS channels is MscL from *Escherichia coli*. A large amount of evidence supports the mechanism that membrane tension in the lipid bilayer directly gates MscL.¹⁶ Due to the small size of *E. coli* cells, generation of giant spheroplasts of *E. coli* has been used to enable direct functional patch-clamp studies of MS channels.²⁵ Reconstituting purified MscL into liposomes for functional characterization has established that no intracellular protein components are required for the gating of MscL and that lipid bilayer tension appears to be the primary stimulus.^{26–28,35} The X-ray crystal structure of an MscL homolog found in *Mycobacterium tuberculosis* has revealed an oligomerized structure³ and further suggested that mutations in the hydrophilicity of a residue within the channel core could alter mechanosensitivity.⁴⁰ In particular, gain-of-function mutants like G22S and G22N exhibit a lower gating threshold tension. These structure–function relationship studies supported that MscL opening is coordinated through integral structural rearrangements. However, despite the strong evidence of membrane tension involvement, a clear understanding of how forces are transmitted from the surrounding lipid bilayer to gate MscL still remains elusive.¹³

An alternative mechanism for MS channel activation proposes that mechanosensitivity involves the connection between the cytoskeleton and MS channels. Since bacterial cytoskeleton is not required for bacterial MS channel function, this mechanism is likely more relevant to animal cells. The importance of the cytoskeleton for activating MS channels has been suggested by several studies.^{29,31} A previous study showed that membrane stress generated by the actin cytoskeleton can gate MS channels in mammalian cells.¹⁴ Although neither MscL nor MscS homologues have been identified in animal and human cells to date, reconstitution of functional MscL activity in mammalian cells was recently demonstrated.⁵ The ability to express MscL in mammalian cells presents new opportunities for studying the activation mechanism of MscL and potentially can introduce new mechanotransduction pathways to mammalian cells.

In this study, we examined MscL function under different mechanical perturbations in mammalian cells. Using adenoviruses, we obtained efficient expression of MscL and confirmed MscL function using an osmotic downshock assay. We performed fluid shear stress experiments to characterize these channels, and found that this failed to gate MscL. Interestingly, using a novel technique, acoustic tweezing cytometry (ATC),⁸ in which acoustically excited lipid-coated microbubbles were targeted to the cell membrane *via* integrin receptors, MscL was robustly gated. Moreover, this ATC-mediated MscL activation was dependent on an intact cytoskeleton and the coupling to integrin receptors. Our results demonstrate that the activation of a bacterial MS channel expressed in mammalian cells can be mediated through localized membrane stress that is dependent on the actin cytoskeleton.

MATERIALS AND METHODS

Adenoviral MscL Expression System in RPE Cells

Constructs for the *E. coli* MscL WT as well as the gain of function mutant, MscL G22S, were kindly provided by Boris Martinac (Victor Chang Cardiac Research Institute, Darlinghurst, Australia). The MscL constructs were subcloned into a tetracycline (tet)-regulatable adenovirus vector using seamless cloning PCR.²¹ His₆-tags were inserted at the N-termini of the MscL sequences for subsequent immunofluorescence imaging and Western blot analysis. All constructs were verified by DNA sequencing at the University of Michigan DNA Sequencing Core. Adenovirus was generated and harvested from human embryonic kidney 293 (HEK293) cells transfected with the pADtet constructs.¹¹ Retinal pigment epithelial (RPE) cells served as the mammalian system for all experiments and were maintained in DMEM/F12 supplemented with 10% fetal bovine serum. To express MscL, RPE cells were co-infected with the adenoviruses containing MscL WT or MscL G22S (an MscL mutant with lower activation threshold) with encoded tet-regulatable promoter and tetracycline transactivator (tTA) adenovirus with incubation duration of 12–16 h prior to all experiments. Addition of tetracycline of various concentrations during infection incubation periods was used to verify proper function of the adenovirus expression system. For immunofluorescence imaging, infected RPE cells were fixed, permeabilized, and labeled with anti-His antibodies (Pierce Antibodies, Rockford, IL). Quantitative analysis of infrared Western Blots was conducted utilizing a LI-COR Odyssey Sa system (Lincoln, Nebraska USA).

Subcellular Fractionation

Cells grown in a 10 cm dish were lysed with 500 μL of subcellular fractionation buffer [250 mM sucrose, 20 mM Hepes (pH 7.4), 10 mM KCl, 1.5 mM MgCl_2 , 1 mM EDTA, 1 mM EGTA, 1 mM DTT, and 1 tablet of cOmplete Protease Inhibitor Cocktail Tablets (Roche)], scraped, and transferred to a microcentrifuge tube. The lysate was passed through a 25G needle 10 times and placed on ice for 20 min. To obtain the nuclear pellet, the tubes were centrifuged at $720\times g$ for 5 min, the supernatant was collected and kept on ice, and the nuclear pellet was washed $1\times$ with the subcellular fractionation buffer. The previously collected supernatant was then spun for 10-min at $10,000\times g$ spin. Supernatant from the $10,000\times g$ spin was further separated by ultracentrifugation at $100,000\times g$ for 1 h, leaving the cytosolic fraction in the supernatant and the membrane fraction in the pellet. All samples were resuspended in SDS sample buffer and MscL expression was detected by Western blot.

Osmotic Shock Experiments

RPE cells were infected with the adenoviruses encoding MscL for 16 h prior the osmotic downshock experiments. Initial pilot experiment was performed by incubating cells for a period of 8 min in 10 mM HEPES and 1 $\mu\text{g}/\text{mL}$ Alexa Fluor 568 phalloidin (Life Technologies, Carlsbad, CA). For the remaining osmotic shock experiments, cells were incubated for a period of 2 min in saline solutions of 10 mM HEPES, 100 μM propidium iodide (PI) (Sigma-Aldrich, St. Louis, MO) and different NaCl concentrations for different osmolarities. PI and phalloidin are both impermeable to the plasma membrane and label the nucleic acids and the actin cytoskeleton respectively upon entering the cells. After incubation, cells were washed with $1\times$ phosphate buffered saline (PBS) twice and fixed with 4% paraformaldehyde. The nucleus was labeled with DAPI after cell permeabilization. PI intensity was quantified and normalized to total cell area in solutions at varying osmolarity. Cell viability was determined by recovery experiments where infected RPE cells were incubated with PI-free, hypo-osmotic solutions of 10 mM HEPES for 2 min, allowed to recover for 2 min in culture medium, and then incubated with $1\times$ PBS containing 100 μM PI for 2 min before fixation and DAPI staining. Imaging was performed on a Nikon TiE inverted microscope system, and image analysis was performed using ImageJ (<http://rsb.info.nih.gov/ij/>).

Shear Flow Experiments

Cells were seeded in μ -slide VI^{0.1} microfluidic channels (ibidi, Verona, WI) overnight prior to infection

with MscL adenoviruses. A 60 mL plastic syringe containing 50 μM propidium iodide in culture medium was mounted to a HA PhD Ultra syringe pump (Harvard Apparatus, Holliston, MA) and connected to the microchannels using sterilized Tygon tubing and Luer fittings. Shear stress in the channels was controlled by varying the flow rate. The shear stress, τ (in dyne/cm^2), as a function of volumetric flow rate, Q (in $\mu\text{L}/\text{min}$), is $\tau = 0.1067Q$ for a fluid viscosity of 0.01 dyne/cm^2 (per manufacturer's application note). Each channel was exposed to a fluid shear stress for 4–5 min. Live cell microscopy was performed on the Nikon Ti-E inverted fluorescence microscope equipped with sCMOS camera (Hamamatsu Photonics, Japan) and controlled via μ Manager software (<http://www.micro-manager.org>).

Acoustic Tweezing Cytometry (ATC) Experiments

A similar ATC setup to one described previously was used in this study.⁸ One day prior to ATC, RPE WT cells were seeded on glass bottom culture dishes (MatTek Corporation, Ashland, MA) coated with 50 $\mu\text{g}/\text{mL}$ fibronectin from human plasma (Sigma-Aldrich, St. Louis, MO). Right before ATC experiments, TargosphereTM-SA microbubbles (Targeson, San Diego, CA) were mixed with biotinylated Arg-Gly-Asp (RGD) peptides (Peptides International, Louisville, KY) for 20 min at room temperature, with a volume ratio of 5:1 of microbubbles ($5 \times 10^8 \text{ mL}^{-1}$) to RGD (0.01 mg/mL). To attach the microbubbles to cells, the culture media from the cell-seeded 35 mm glass bottom dish was removed followed by immediate addition of 20 μL of microbubble–RGD mixture. The small fluid volume permitted inversion of the culture dish to allow microbubbles to float upward and facilitate their attachment to the cells via RGD–integrin bindings. After 10 min, the dish was flipped back and unbound microbubbles were removed by a gentle wash with culture media.

During experiments, the cell-seeded dish was placed on a 37 °C heated stage on an inverted microscope (Eclipse Ti-U; Nikon, Melville, NY). A 40 \times objective (0.75 NA) was used for observation of cells and microbubble activities. A 10 MHz focused transducer (Olympus, Waltham, MA) was positioned at an incident angle of 45° to apply ultrasound pulses to excite the microbubbles attached to the cells. The transducer was driven by a waveform generator (33250A; Agilent Technologies, Palo Alto, CA) and a 75 W power amplifier (75A250; Amplifier Research, Souderton, PA). The ultrasound pulses applied in this study each had fixed pulse duration (PD) of 50 ms and pulse repetition frequency (PRF) of 5 Hz. The total duration of ultrasound application was 10 s with the acoustic pressure amplitude of the ultrasound pulses as a variable. The free field acoustic pressure was measured

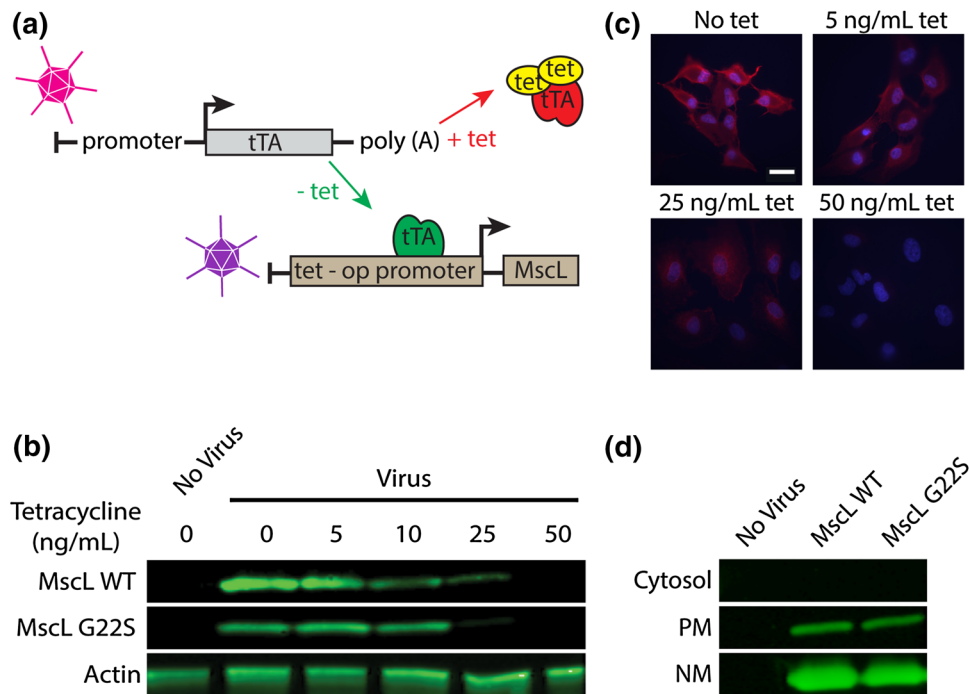


FIGURE 1. Viral expression system for mammalian cells. (a) An adenovirus-based system for tetracycline-controlled transcriptional activation of MscL expression which consists of co-infection of tetracycline transactivator (tTA) and MscL viruses. In the absence of tet, tTA binds to the tet-op promoter upstream of the MscL gene and induces expression. In the presence of tet, tTA is sequestered, inhibiting expression of MscL. (b) Western blot analysis of infected whole cells and (c) fluorescent images of immunostained His₆-tagged MscL in mammalian cells cultured at different concentration of tetracycline. Scale bar = 25 μm. (d) Western blot analysis of fractionated cells showing MscL subcellular localization. Note that a direct comparison of the levels of expression cannot be made because the strong western blot bands of MscL in the nuclear membrane was due to more concentrated fraction compared to the plasma membrane fraction.

using a 40 μm calibrated needle hydrophone (HPM04/1; Precision Acoustics, UK). The application of ultrasound was synchronized with a high-speed camera (FASTCAM SA1; Photron, San Diego, CA), which was used to capture the ultrasound-driven microbubble activities at a frame rate of 5000 frames/s. The translational displacement and the radius of the microbubbles before, during, and after ultrasound application were obtained from the high-speed image sequences using a custom MATLAB program. Only cells with bound microbubbles that had visible movements during ultrasound pulses were included in our quantitative analysis.

RESULTS

Expression of Bacterial MscL in Mammalian Cells

We first sought to develop a viral-based strategy for introducing MscL into mammalian cells (Fig. 1a). WT and mutant MscL constructs with N-terminal His₆-tag were cloned into a tetracycline-regulatable adenoviral vector. Infection with MscL-containing and

tetracycline transactivator (tTA)-containing adenoviruses enabled high expression efficiencies compared to transient transfection by using DNA vectors. Addition of tetracycline (tet) can tune the protein expression level by sequestering tTA. MscL expression in RPE cells infected with the adenoviruses containing MscL WT or MscL G22S exhibited a tetracycline dose dependence, as detected by both Western blot (Fig. 1b), and immunofluorescence (Fig. 1c). Nearly all the cells were infected and expressed MscL, and 50 ng/mL of tet was sufficient to turn off MscL expression. This experiment also served to validate our viral-based expression system for introducing MscL to mammalian cell lines. Since the His₆-tag is present on the cytoplasmic side of MscL, cells were permeabilized for immunofluorescence examination. Interestingly, in addition to staining the plasma membrane, staining of MscL near the nucleus was observed. To further confirm this observed localization of MscL, cell fractionation was performed and MscL was found in both plasma membrane and the nucleus (Fig. 1d). It was not immediately clear whether MscL was inserted in the double lipid bilayer of the nuclear envelope or just to the outer lipid bilayer of the nucleus.

Activation of MscL by Increasing Membrane Tension using Osmotic Shock

In *E. coli* subjected to an osmotic downshock, MscL and MscS allow solutes to be released while maintaining cell viability. Indeed it has been shown that cells with double null mutants are osmotically fragile.¹⁹ In addition to this, reconstitution of MscL into liposomes has demonstrated that MscL responds to membrane tension alone, and does not require any other proteins.^{12,32} To determine if MscL introduced in mammalian cells can be gated similarly by osmotic pressure, we first tested if hypo-osmotic solution could gate MscL with fluorescent phalloidin included in the medium. The large size of MscL's open pore allows free passage of large organic osmolytes. Rhodamine dye conjugated phalloidin is ~1590 Da and binds strongly to filamentous actin (F-actin) and not to monomeric actin. It fluorescently labels the F-actin and is non-fluorescent when not bound to actin. Using this assay, we found that RPE cells not expressing MscL had no phalloidin staining under both iso-osmotic and hypo-osmotic (10 mM HEPES) conditions for a period of 8 min, as expected (Fig. 2a). In RPE cells expressing MscL, strong phalloidin staining was observed for those subjected to the hypo-osmotic condition but not the iso-osmotic condition. Together, these results confirmed the functional expression of MscL in RPE cells. Previous work by Doerner *et al.*¹⁴ showed that chemically-induced activation of MscL G26C was cytotoxic for periods of ≥ 10 min; and that 2 min was sufficient to allow uptake of fluorescent molecules on the order of 800 Da. For subsequent osmotic pressure experiments, we used propidium iodide (PI; 668 Da) and shortened osmotic pressure incubation times to 2 min. First, to assess the viability of the MscL expressing cells subjected to hypo-osmotic conditions and assure that dye uptake was due to channel activation and not cell death, PI was added to the cells during and after osmotic downshock (Fig. 2b). PI is an impermeable, intercalating molecule that has a detectable increase in fluorescence when bound to nucleic acids after entering cells. This dye is often used to assess cell viability because, due to its small size, it enters dying cells quickly. Because MscL is a non-selective channel that can allow the passage of molecules up to 6.5 kDa, PI should be able to also transit through the opened MscL in non-dying cells.³⁶ When PI was added to the MscL WT expressing cells during osmotic downshock, PI uptake was observed, as expected. In contrast, there was no PI uptake when PI was added to both MscL WT and MscL G22S after the cells had been subjected to osmotic downshock and recovered in iso-osmotic solution, confirming that the cell via-

bility was maintained during osmotic downshock and dye uptake was due to MscL activation.

To further investigate the responsiveness of MscL activation by osmotic pressure and to determine the threshold of MscL activation, we conducted PI uptake experiments under different osmotic conditions. For MscL expressing cells some dye uptake was evident at 100 mOsm and the influx continued to increase with decreasing solution osmolarity. As expected and consistent with the earlier result, no PI uptake was detected at any osmolarity when RPE cells did not express MscL (Figs. 2c and 2d). At the low end of the osmolarity, cells expressing MscL G22S took up significantly more PI than MscL WT cells. Interestingly, it appeared that MscL WT had a lower activation threshold than MscL G22S.

Fluid shear stress was unable to activate MscL

Mechanochemical signal transduction by shear-sensitive mechanoreceptors allows sensing of hemodynamic forces, particularly in endothelial cells.³⁸ We next asked whether shear stress associated with globally applied fluid flow could possibly activate MscL in mammalian cells. This experiment has not been possible because of the limitations of exerting shear stress to *E. coli* or spheroplasts. We controlled shear stress in our experiments using microfluidic channels with well-defined geometry (Fig. 3a). The cultured cells in microchannels expressed functional MscL that responded to osmotic downshock (Figs. 3b and 3c). However, no robust MscL activation was detected in cells subjected to shear stress up to 400 dyne/cm² (Fig. 3d). At 400 dyne/cm² of shear stress, a few cells expressing MscL G22S were observed with PI uptake, but cell detachment became evident when shear stress ≥ 400 dyne/cm² was applied, as others have shown.³⁰

Localized Stress by Acoustic Tweezing Cytometry (ATC) Activates MscL

Because of the fluidity of the lipid bilayer membrane, flow-generated shear stress is unable to exert forces directly to the lipid molecules to induce membrane tension. Shear deformation becomes relevant if the membrane is coupled to structures such as the cytoskeleton. To test if localized stress to the cells could potentially induce activation of MscL expressed in mammalian cells, we conducted a series of experiments using ATC (Fig. 4a). ATC uses ultrasound pulses to actuate gas-filled microbubbles that were functionalized with Arg-Gly-Asp (RGD) peptide and attached to integrin receptors of the cells. Ultrasound pulses generate a directional force, the acoustic radiation force,⁴

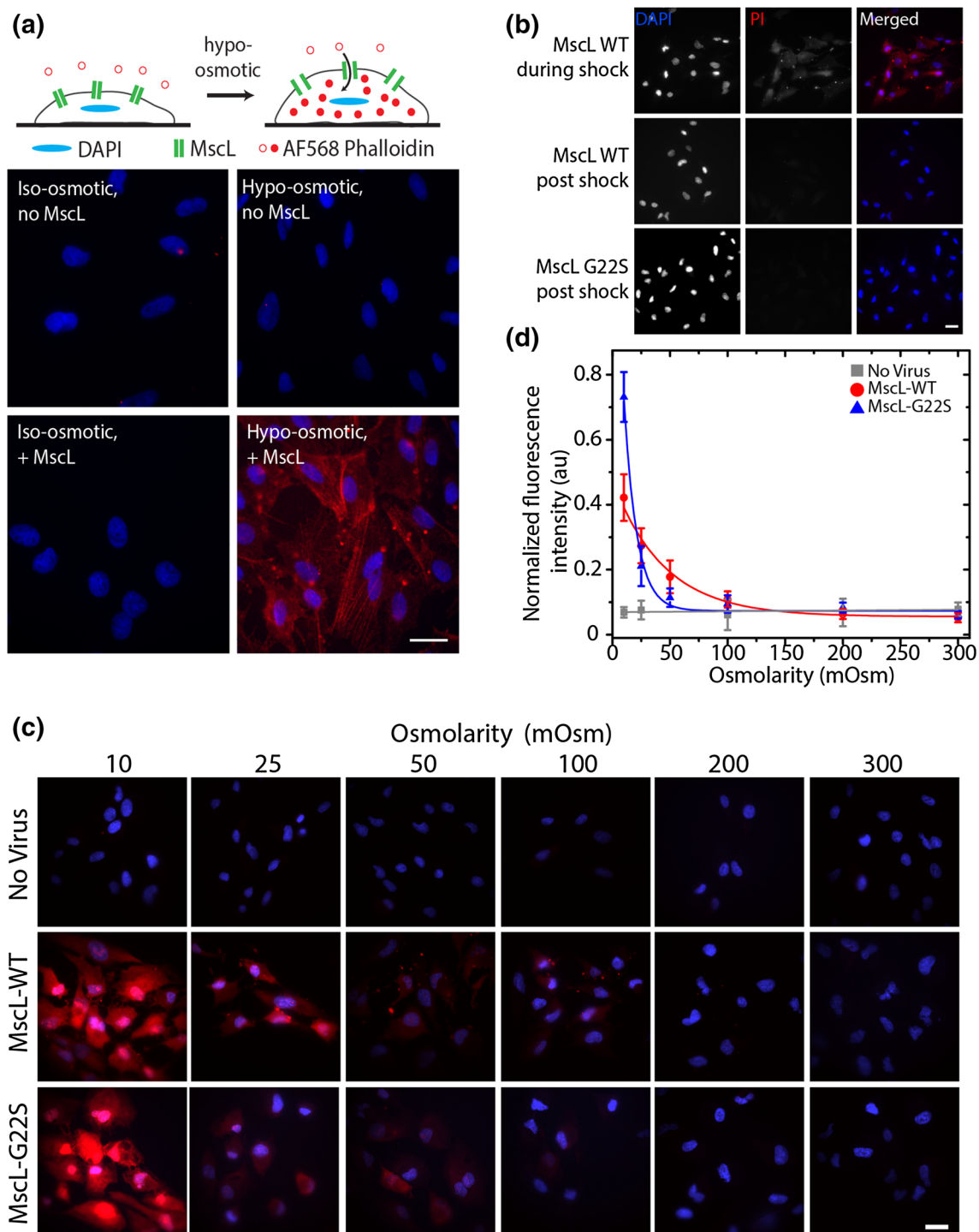


FIGURE 2. Osmotic downshock experiments in MscL expressing RPE cells. (a) Cartoon description of osmotic shock assay (top). Under hypo-osmotic conditions, mammalian cell membranes swell leading to increased membrane tension and MscL activation, which allows for uptake of fluorescent phalloidin. Fluorescent images of fixed, MscL WT infected and non-infected cells incubated under iso-osmotic (300 mOsm) and hypo-osmotic (10 mOsm) solution containing fluorescent phalloidin for 8 min (bottom). F-actin labeling is shown in red and DAPI labeling in blue. (b) Fluorescent images of infected cells incubated in hypo-osmotic solution for 2 min. MscL WT cells were incubated with PI during hypo-osmotic shock, and both MscL WT and G22S expressing cells were incubated with PI after a 2 min recovery period in medium post hypo-osmotic shock. (c) Fluorescent images showing PI uptake in non-infected cells and cells expressing MscL WT and G22S. (d) Average PI uptake after 2 min incubation with PI-containing saline solutions of decreasing osmolarity ($n_{\text{expt}} = 3$, $n_{\text{cell/expt}} \sim 100$). All scale bars = 25 μm . Error bars are standard error of the mean.

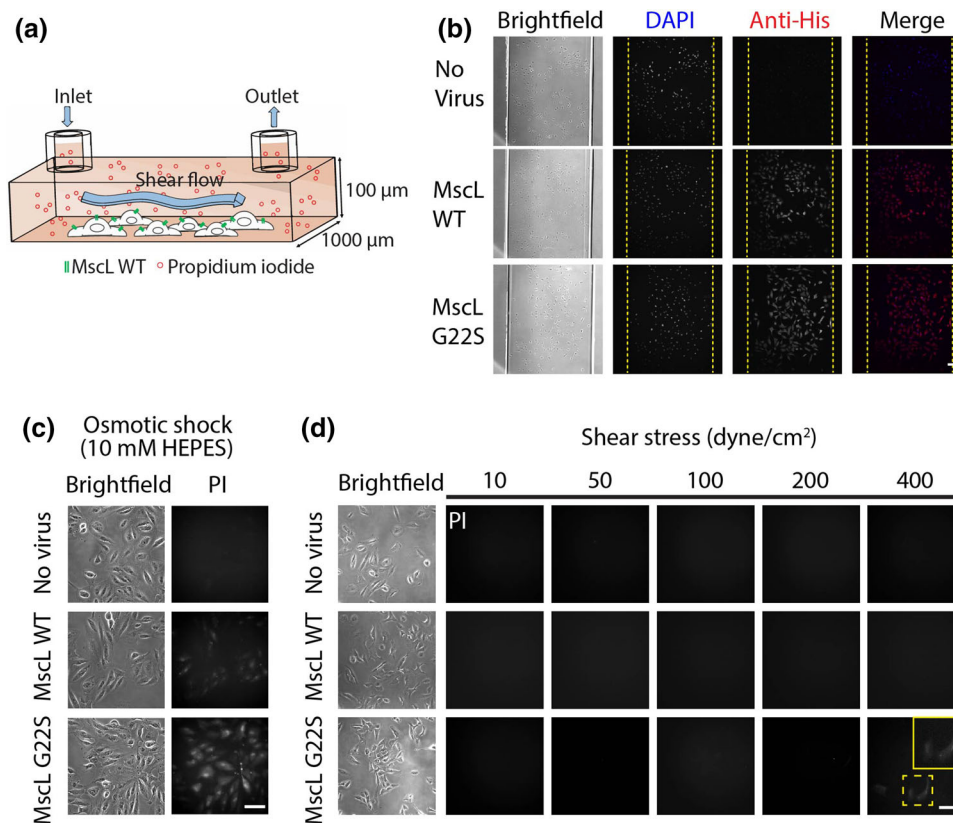


FIGURE 3. Flow induced shear stress for activation of MscL in mammalian cells in microfluidic channels. (a) Cartoon showing shear flow of medium containing PI on MscL infected cells seeded in microfluidic channels. (b) Brightfield and immunofluorescent images of non-infected, MscL WT, and MscL G22S infected cells in microfluidic channels. DAPI and anti-His were used to stain for the cell nucleus and His-tagged MscL respectively. Scale bar = 100 μm . (c) Brightfield and fluorescent images of PI uptake for no virus, MscL WT, and MscL G22S infected cells incubated in PI-containing hypo-osmotic solution for 2–4 min in microfluidic channels. (d) Brightfield and fluorescent images of PI uptake for no virus, MscL WT, and MscL G22S infected cells subjected to different shear stresses for 4–5 min in microfluidic channels. Inset (yellow solid box) in MscL G22S 400 dyne/cm² panel shows enlarged image of cells with PI uptake (yellow dashed box). Scale bars = 25 μm for (c, d).

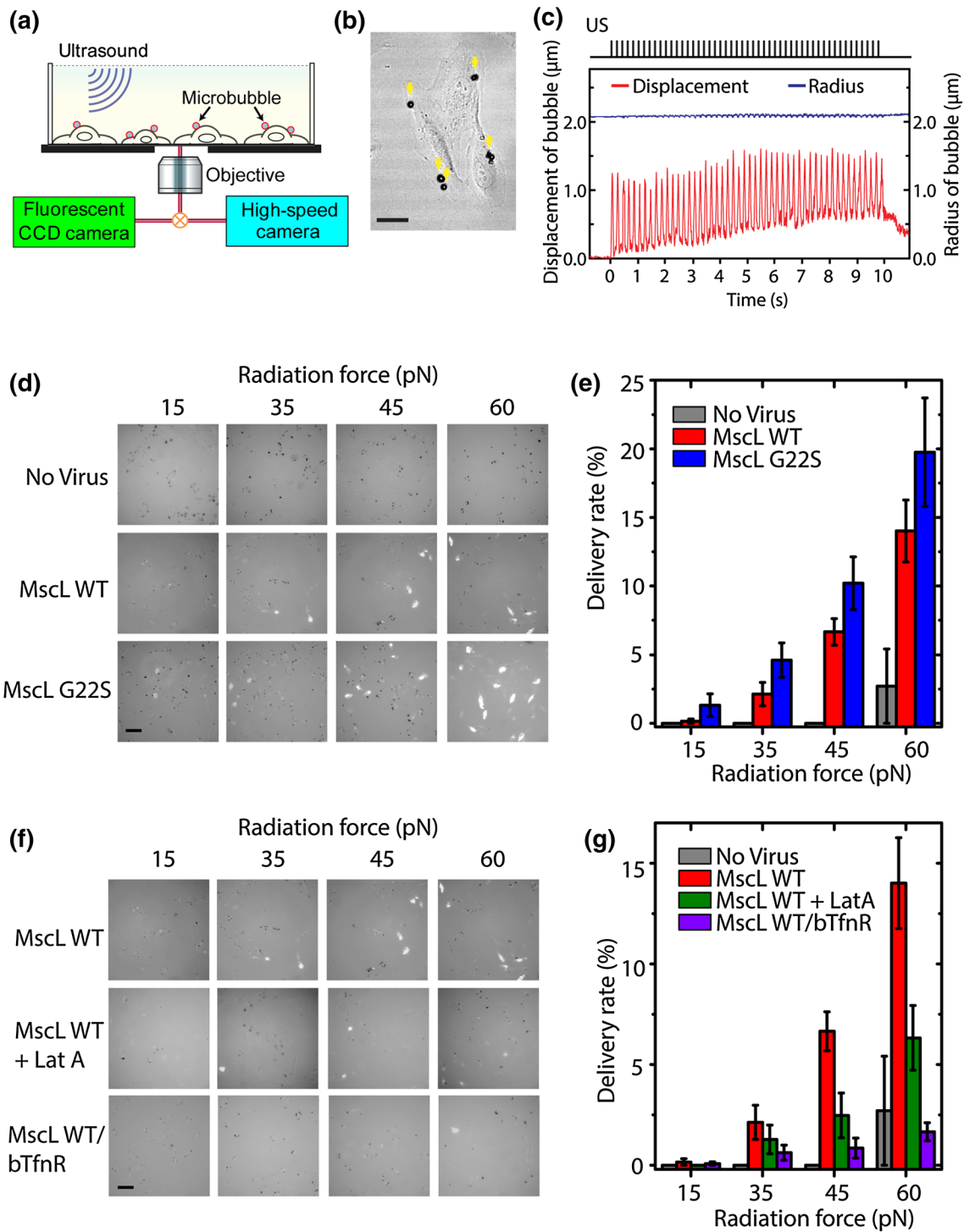
on the microbubbles, and the displacement of the integrin-anchored microbubbles from their original location leads to targeted stress to the cells through the microbubble-integrin-cytoskeleton linkage. In addition, ultrasound application readily generates cavitation of the microbubbles (rapid volume expansion and contraction), which induced microstreaming of fluid, thus shear stress, near the microbubbles.²² Our previous work has shown that ATC using ultrasonic excitation of RGD-functionalized microbubbles bound to integrins elicited strong cytoskeleton contractile responses that requires an intact actin cytoskeleton and Rho/ROCK signaling.⁸

In this study, functionalized microbubbles were introduced to cells seeded on a glass-bottomed culture dish such that 3.7 ± 2.2 ($n = 40$ cells) microbubbles were attached to each of the cells (Fig. 4b). Using a 10 MHz transducer mounted at a 45° angle, microbubbles were subjected to 10 s application of ultrasound pulses with a duty cycle of 25% and PRF

of 5 Hz. These parameters minimized the cavitation effect (thus the localized shear stress from microstreaming) compared to the directional force (acoustic radiation force) exerted on the microbubbles. The primary acoustic radiation force was generated by the incident ultrasound field on a microbubble *via* momentum transfer, and can be calculated as⁴

$$F = \frac{2\pi P_A^2 R_0}{\rho_0 c \omega} \frac{\delta_{\text{tot}} \omega_0 / \omega}{((\omega_0 / \omega)^2 - 1)^2 + (\delta_{\text{tot}} \omega_0 / \omega)^2},$$

where P_A is the acoustic pressure amplitude, R_0 is the equilibrium radius of the microbubble, δ_{tot} is the total damping constant (0.1), ρ_0 is the medium density (1000 kg/m³), and c is the speed of sound in medium (1500 m/s), $\omega_0 = 2\pi f_0$, where f_0 is the resonance frequency (3.5 MHz) of the lipid-coated microbubble with a radius of 2 μm ,⁹ and ω is the frequency of the ultrasound applied (10 MHz). Using pressure amplitude between 0.047 MPa and 0.095 MPa, forces between 15 and 60 pN can be generated on a microbubble (Supplemental Fig. S1).



Large amplitude expansion/contraction of microbubbles (strong cavitation), which typically occurs under high acoustic pressures or when the frequency of the incident ultrasound field is close to the resonant frequency of the microbubbles, can lead to transient membrane disruption by sonoporation that permits transport of exogenous molecules.⁷ Large amplitude

cavitation often leads to reduction in microbubble size over time, due to gas leakage from the disrupted protective lipid layer of the encapsulated microbubbles. To ensure cavitation was not the cause for PI uptake by disrupting the cell membrane in our experimental study, we employed relatively low acoustic pressure amplitudes and 10 MHz center frequency, which was

◀ **FIGURE 4. Acoustic tweezing cytometry for activation of MscL in mammalian cells and uptake of impermeable molecules.** (a) Experimental setup of ultrasound excitation of targeted microbubbles attached to the membrane of cells (drawing not to scale). (b) Brightfield image of RPE cells with attached RGD functionalized microbubbles indicated by yellow arrows. (c) Ultrasound- (US) induced microbubble activities. Typical translational displacement and radius profile of a microbubble during the 10-s US stimulation (pulse duration = 50 ms, PRF = 5 Hz, Acoustic pressure = 0.071 MPa). (d) Fluorescent images of MscL WT, MscL G22S, and non-infected cells with RGD-microbubbles subjected to different radiation forces. Cells with PI uptake after US application exhibit bright fluorescence. (e) Delivery rate (percentage of cells with PI uptake after US application) of MscL WT, MscL G22S, and non-infected cells with integrin-bound, RGD-microbubbles ($n_{\text{expt}} = 3-5$, $n_{\text{cell}} = 100-400$). (f) Fluorescent images showing PI uptake after US application for MscL WT infected cells not treated and treated with 50 nM latrunculin A with RGD-microbubbles, and cells infected with MscL WT and bTfnR adenoviruses with avidin functionalized microbubbles bound to biotinylated-transferrin receptors. (g) Delivery rate for MscL WT infected cells not treated and treated with 50 nM latrunculin A with integrin-bound microbubbles and MscL/bTfnR infected cells with biotinylated-transferrin receptor-bound microbubbles ($n_{\text{expt}} = 3$, $n_{\text{cell}} = \sim 100-300$). Scale bars = 25 μm for (b, d, f). One-tailed *t* test comparing MscL-expressing vs. non-infected cells showed significant differences between all conditions ($p < 0.05$), except for 15 pN. Error bars are standard error of the mean.

far away from the microbubble resonant frequency. High-speed imaging confirmed that microbubble expansion and contraction was minimal (<5% of the equilibrium radius) and the size of microbubbles remained stable throughout ultrasound application (Fig. 4c). Furthermore, experiments with PI in the medium showed no uptake in non-expressing cells with and without microbubbles, nor MscL expressing cells without microbubbles, indicating no cell membrane disruption by ultrasound application. Translational displacement of the microbubbles was observed with an average displacement of $\sim 1 \mu\text{m}$ achieved during each ultrasound pulse. During the pulse-off period, the microbubbles partially returned to their original positions, dictated by the elastic properties of the microbubble-focal adhesion-cytoskeleton linkages. Besides possible cell remodeling, the creep in the displacements may be due to the short time interval between pulses such that there may not be enough time for a full recovery of microbubble displacements.

Interestingly, with the use of ATC to apply forces to the integrin receptors, cells expressing MscL clearly took up PI as the acoustic radiation force increased from 0 to 60 pN, in contrast to uninfected cells without visible PI uptake (Fig. 4d), indicating gating of the MscL expressed in the cells by ATC stimulation. The percentage of MscL G22S expressing cells that took up PI increased to up to about 20%, which was higher than the percentage of cells with PI uptake of MscL WT cells (about 14%), consistent with the lower tension threshold for MscL G22S (Fig. 4e).

To exclude the possibility that virus-infection of cells somehow caused the cells to become more sensitive to ATC perturbation, we tested whether RPE cells expressing adenovirus-encoded biotinylated transferrin receptor (bTfnR) using a site-specific labeling approach developed previously²⁰ with RGD bound microbubbles would take up PI when subjected to ATC stimulation. We found that bTfnR expressing RPE cells did not take up PI at any applied forces by ATC, indicating that the viral infection had no effect on PI uptake. As RGD-functionalized microbubbles were targeted to integrin receptors, we tested whether MscL activation could occur by forces applied to other membrane receptors such as bTfnR. With microbubbles bound to bTfnR on cells expressing both bTfnR and MscL, we found no PI uptake when subjected to the same ATC stimulation (Fig. 4f), suggesting that force transduction through the integrin-focal adhesion complex is critical for the observed activation of MscL and PI uptake by ATC stimulation. Consistent with this, mild disruption of the actin cytoskeleton by treating the cells with 50 nM of latrunculin A, an actin monomer binding drug, reduced the PI delivery efficiency significantly at all forces (Fig. 4g). Together, these results showed that the observed activation of MscL is mediated through localized mechanical stress induced by ultrasound actuation of integrin-anchored microbubbles on the cells, which pull on the microbubble-integrin-cytoskeleton linkages, in an actin-dependent manner.

DISCUSSION

Mechanosensation is one of the most ubiquitous phenomena in living systems and MS channels constitute the simplest mechanism of mechanotransduction.¹³ However, our understanding of MS channels is far from complete. Studies of mechanosensation in bacteria have led to the discovery of MS channels that gate by lipid bilayer tension; while identification of the gating mechanisms of MS channels in eukaryotes has been much more challenging due to the rarity of certain sensory cells and the difficulty in assaying the function of candidate mechanotransduction molecules.² Our results presented in this study identified a new activation mechanism for gating MscL in a different cellular context, by employing a new cellular mechanics tool (ATC) on mammalian cells expressing bacterial MscL.

Our finding that MscL was localized to nuclear membrane of the infected RPE cells, in addition to the plasma membrane, and possibly also to other cellular compartments, is interesting. This may not be entirely surprising given that MscL does not have a leader

sequence targeting it specifically to the plasma membrane. Thus it may be able to insert into any cellular membranes as it readily inserts into liposome bilayers, leading to interesting consequences. For example, expression of MscL in mammalian cells was found in this study to permit the influx of small molecules such as PI and phalloidin across the plasma membrane during osmotic downshock.

In cells expressing MscL G22S, significantly higher PI uptake was observed with the strongest osmotic downshock tested compared to MscL WT, but the threshold osmolarity for gating MscL appears to be higher (lower osmolarity) for MscL G22S than for MscL WT. Potentially, there could be differences in the activation of the two MscL molecules that resulted in different opening states. A possible mechanism is the “silent expansion” of MscL prior to opening of the channel pore.³³ Given that MscL G22S is more sensitive to tension, it may silently expand sooner than WT MscL, which in turn would relax membrane tension due to the low osmolarity. This would result in MscL G22S appearing to open at a higher osmolarity threshold than MscL WT.

Our experiments showed that MscL in RPE cells was not sensitive to globally applied flow-induced shear stress up to 400 dyne/cm². At 400 dyne/cm², a surface tension of up to 0.1 mN/m could be induced to a 25 μ m cell, but this surface tension was much lower than the reported ~12 mN/m for MscL activation.³⁵ Thus, the inability for globally applied fluid shear stress to open MscL in our experiment may be primarily due to the insufficient membrane tension required to gate MscL that is produced by fluid flow. However, increasing the flow velocity to increase shear stress was not feasible in our experiments due to cell detachment at higher flow rates, indicating the limitation of the use of flow-induced shear stress as a robust mechanism for gating of MscL expressed in RPE cells. As such, shear-sensitive MS channels could have a very different gating mechanism than sensing pure membrane tension induced globally as the primary stimulus. For example, tethering to the cytoskeleton may be important in the activation mechanism for shear-sensitive MS channels.

MS channel gating is employed in hair cells and neuronal cells, which have a direct connection between the channels and the cytoskeleton and/or extracellular matrix (ECM) in order to confer directional sensitivity.^{2,39} Furthermore, a recent work postulates that stiffened lipid platforms that can direct, rescale, and confine force may be a plausible mechanism that is used by mammalian cells.¹ This is an interesting possibility because cell membranes are highly heterogeneous and cells have extensive cytoskeleton networks that connect to the ECM through transmembrane

integrin receptors. Since the cytoskeleton-membrane interaction plays a key role in regulating membrane properties, cytoskeleton and ECM may serve to modulate the dynamic range of MS channel gating.²⁴ The use of the novel ATC technique in this study for applying localized mechanical forces with subcellular resolution provided the opportunity to investigate the involvement of this mechanism in MscL gating. Our finding that local force application using ATC could open MscL in an actin-dependent and integrin-dependent manner supports this idea, and is consistent with a previous study that showed direct mechanical stimulation of actin stress fibers activates MS channels in endothelial cells; where a stretching force of 5.5 pN exerted on stress fibers resulted in inward current from MS channels.¹⁴

In this study and indicated by previous work, ATC applied local mechanical stresses to the cells *via* acoustic actuation of integrin-bound microbubbles. Although the detailed process of force generation on the cells is the focus of an on-going investigation, it is clear that the displacements of the integrin-bound microbubbles by the acoustic radiation force are involved in the stress exerted to the cells. On the other hand, fluid microstreaming induced by a cavitating microbubble attached to a cell during ultrasound application can also exert localized shear stress on the nearby cells, as demonstrated previously.²² The effect of the localized shear stress by cavitation-induced microstreaming will be further investigated in future studies. However, in this study, the use of low acoustic pressures and center frequency of 10 MHz, far above the bubble resonant frequency, aimed to reduce the impact of cavitation relative to microbubble displacements. While the force that we applied to the microbubbles corresponding to activation of MscL ranged from 30 to 60 pN, how this force is translated to the cells to contribute to gating MscL requires further investigation. In addition, the effects of the number of microbubbles and duration of ATC stimulation will need to be elucidated.

Nonetheless, the forces we applied to cells by the use of ATC to open MscL is greater than the ~5 pN drag force that is exerted by a globally applied shear stress of 400 dyne/cm², assuming a protein of 5 nm in diameter. Assuming a microbubble has a contact diameter with the cell membrane of 250 nm, a membrane tension of ~12 mN/m, comparable to the MscL activation tension, can be generated by a radiation force of 60 pN. We believe it is the localized force transduction *via* the microbubble-integrin-actin cytoskeleton that was critical for the gating of MscL. The finding that exerting the same force using ATC on microbubbles targeted to bTfnR did not gate MscL supports the idea that force transduction *via* integrin-actin cytoskeleton

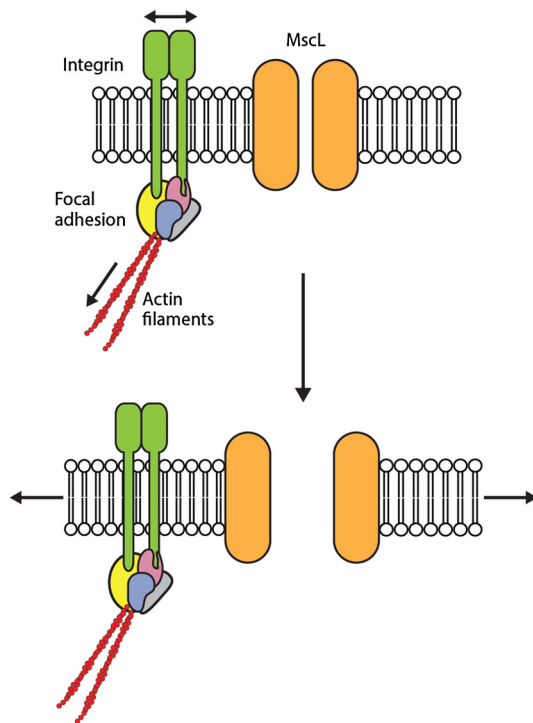


FIGURE 5. Model for actin cytoskeleton-mediated MscL activation in mammalian cells. Forces exerted onto integrins linked to focal adhesion and intact actin cytoskeleton (top) can generate sufficient membrane tension to activate untethered MscL (bottom).

is responsible for the observed MscL gating. Interestingly, there are no known molecular interactions between MscL and any mammalian cellular components, thus force transduction *via* the cytoskeleton is highly unlikely to act through a direct tethering mechanism that has been proposed to pre-stress MS channels and affects their sensitivity.³⁴ Instead, we believe that a local change in membrane tension was generated by ATC and gated MscL in our experiments, revealing a new mechanism for gating MscL in mammalian cells.

Our ATC experiment also provides the first demonstration where delivery of molecules across the cell membrane can be achieved through the activation of a non-selective MS channel, without transient membrane disruption through sonoporation, providing a promising method for intracellular molecular delivery. Since microbubbles interact with ultrasound very efficiently and have been successfully used clinically as an imaging contrast agent for echocardiography,^{10,17} and they can be easily removed from the cells leaving no exogenous material behind, the use of ultrasound in ATC is advantageous as it can exert forces on multiple cells simultaneously *via* biocompatible and multifunctional microbubbles in both 2D or 3D settings with a force range that is compatible with biological studies. Our

results reported in this study demonstrate a new platform for further investigating MscL gating under different cellular conditions. In addition to this, the ATC experiment results support a new cytoskeleton-dependent mechanism for MscL activation. Despite MscL not being directly tethered to the actin cytoskeleton, localized force application *via* the integrin-focal adhesion-cytoskeleton linkage can generate sufficient membrane tension to activate MscL (Fig. 5). This represents a hybrid model that combines elements of the bilayer tension model and the cytoskeleton-tethered model, where the actin cytoskeleton force transduction can mediate activation of membrane tension responsive channels such as prokaryotic MscL. However, it is unclear how exactly the integrin-focal adhesion-cytoskeleton linkage generates the required membrane tension to open MscL.

The ability to functionally express MscL in mammalian cells could provide new opportunities for mechanobiology studies. MscL expression in non-mechanosensitive cells can render them mechanosensitive and be used as a novel mechanism for controlled molecular delivery in these cells. A number of diseases such as muscular dystrophy, sickle cell anemia, and cardiac arrhythmias have been linked to defects in activating MS channels.³⁴ Thus, it is enticing to suggest that engineered MscL with precise gating behaviors could be used as a therapeutic tool. Finally, one could also imagine the potential of using MscL in building functional cellular devices that are mechanosensitive.

ELECTRONIC SUPPLEMENTARY MATERIAL

The online version of this article (doi:10.1007/s12195-014-0337-8) contains supplementary material, which is available to authorized users.

ACKNOWLEDGMENTS

We would like to thank Dr. Boris Martinac for the *E. coli* MscL constructs used in this study, and his very thoughtful feedback on our manuscript. We thank the Liu lab for helpful discussions and Dr. Jianping Fu for use of his lab for some experiments in the study. J.H. was supported by the NIH's Microfluidics in Biomedical Sciences Training Program: NIH NIBIB T32 EB005582. A.P.L. and V.L.M. were supported by the NIH Director's New Innovator Award: NIH DP2 HL117748-01. C.X.D. and D.C. were supported by funding from the Department of Biomedical Engineering at the University of Michigan. The authors declare no conflict of interests.

CONFLICT OF INTEREST

J. Heureaux, D. Chen, V.L. Murray, C.X. Deng, and A.P. Liu declare that they have no conflicts of interests.

ETHICAL STANDARDS

No human studies were carried out by the authors for this article. No animal studies were carried out by the authors for this article.

REFERENCES

- ¹Anishkin, A., and C. Kung. Stiffened lipid platforms at molecular force foci. *Proc. Natl Acad. Sci. U.S.A.* 110:4886–4892, 2013.
- ²Chalfie, M. Neurosensory mechanotransduction. *Nat. Rev. Mol. Cell Biol.* 10:44–52, 2009.
- ³Chang, G., R. H. Spencer, A. T. Lee, M. T. Barclay, and D. C. Rees. Structure of the MscL homolog from *Mycobacterium tuberculosis*: a gated mechanosensitive ion channel. *Science* 282:2220–2226, 1998.
- ⁴Dayton, P. A., K. E. Morgan, A. L. Klibanov, G. Brandenburger, K. R. Nightingale, and K. W. Ferrara. A preliminary evaluation of the effects of primary and secondary radiation forces on acoustic contrast agents. *IEEE Trans. Ultrason. Ferroelectr. Freq. Control* 44:1264–1277, 1997.
- ⁵Doerner, J. F., S. Febvay, and D. E. Clapham. Controlled delivery of bioactive molecules into live cells using the bacterial mechanosensitive channel MscL. *Nat. Commun.* 3:990, 2012.
- ⁶Evans, E. A., and D. A. Calderwood. Forces and bond dynamics in cell adhesion. *Science* 316:1148–1153, 2007.
- ⁷Fan, Z., H. Liu, M. Mayer, and C. X. Deng. Spatiotemporally controlled single cell sonoporation. *Proc. Natl. Acad. Sci. U.S.A.* 109:16486–16491, 2012.
- ⁸Fan, Z., Y. Sun, C. Di, D. Tay, W. Chen, C. X. Deng, and J. Fu. Acoustic tweezing cytometry for live-cell subcellular modulation of intracellular cytoskeleton contractility. *Sci. Rep.* 3:2176, 2013.
- ⁹Goertz, D. E., N. de Jong, and A. F. W. van der Steen. Attenuation and size distribution measurements of definity and manipulated definity populations. *Ultrasound Med. Biol.* 33:1376–1388, 2007.
- ¹⁰Goldberg, B. B., J. B. Liu, and F. Forsberg. Ultrasound contrast agents: a review. *Ultrasound Med. Biol.* 20:319–333, 1994.
- ¹¹Hardy, S., M. Kitamura, T. Harris-Stansil, Y. Dai, and M. L. Phipps. Construction of adenovirus vectors through Cre-lox recombination. *J. Virol.* 71:1842–1849, 1997.
- ¹²Hase, C. C., A. C. Le Dain, and B. Martinac. Purification and functional reconstitution of the recombinant large mechanosensitive ion channel (MscL) of *Escherichia coli*. *J. Biol. Chem.* 270:18329–18334, 1995.
- ¹³Haswell, E. S., R. Phillips, and D. C. Rees. Mechanosensitive channels: what can they do and how do they do it? *Structure* 19:1356–1369, 2011.
- ¹⁴Hayakawa, K., H. Tatsumi, and M. Sokabe. Actin stress fibers transmit and focus force to activate mechanosensitive channels. *J. Cell Sci.* 121:496–503, 2008.
- ¹⁵Ingham, K. C., S. A. Brew, S. Huff, and S. V. Litvinovich. Cryptic self-association sites in type III modules of fibronectin. *J. Biol. Chem.* 272:1718–1724, 1997.
- ¹⁶Iscla, I., and P. Blount. Sensing and responding to membrane tension: the bacterial MscL channel as a model system. *Biophys. J.* 103:169–174, 2012.
- ¹⁷Kaul, S. Myocardial contrast echocardiography: a 25-year retrospective. *Circulation* 118:291–308, 2008.
- ¹⁸Krammer, A., D. Craig, W. E. Thomas, K. Schulten, and V. Vogel. A structural model for force regulated integrin binding to fibronectin's RGD-synergy site. *Matrix Biol.* 21:139–147, 2002.
- ¹⁹Levina, N., S. Totemeyer, N. R. Stokes, P. Louis, M. A. Jones, and I. R. Booth. Protection of *Escherichia coli* cells against extreme turgor by activation of MscS and MscL mechanosensitive channels: identification of genes required for MscS activity. *EMBO J.* 18:1730–1737, 1999.
- ²⁰Liu, A. P., F. Aguet, G. Danuser, and S. L. Schmid. Local clustering of transferrin receptors promotes clathrin-coated pit initiation. *J. Cell Biol.* 191:1381–1393, 2010.
- ²¹Lu, Q. Seamless cloning and gene fusion. *Trends Biotechnol.* 23:199–207, 2005.
- ²²Marmottant, P., and S. Hilgenfeldt. Controlled vesicle deformation and lysis by single oscillating bubbles. *Nature* 423:153–156, 2003.
- ²³Martinac, B. Mechanosensitive ion channels: molecules of mechanotransduction. *J. Cell Sci.* 117:2449–2460, 2004.
- ²⁴Martinac, B. The ion channels to cytoskeleton connection as potential mechanism of mechanosensitivity. *Biochim. Biophys. Acta* 1838(2):682–691, 2013.
- ²⁵Martinac, B., M. Buechner, A. H. Delcour, J. Adler, and C. Kung. Pressure-sensitive ion channel in *Escherichia coli*. *Proc. Natl. Acad. Sci. U.S.A.* 84:2297–2301, 1987.
- ²⁶Moe, P., and P. Blount. Assessment of potential stimuli for mechano-dependent gating of MscL: effects of pressure, tension, and lipid headgroups. *Biochemistry* 44:12239–12244, 2005.
- ²⁷Nomura, T., C. G. Cranfield, E. Deplazes, D. M. Owen, A. Macmillan, A. R. Battle, M. Constantine, M. Sokabe, and B. Martinac. Differential effects of lipids and lyso-lipids on the mechanosensitivity of the mechanosensitive channels MscL and MscS. *Proc. Natl. Acad. Sci. U.S.A.* 109:8770–8775, 2012.
- ²⁸Perozo, E., A. Kloda, D. M. Cortes, and B. Martinac. Physical principles underlying the transduction of bilayer deformation forces during mechanosensitive channel gating. *Nat. Struct. Biol.* 9:696–703, 2002.
- ²⁹Savage, C., M. Hamelin, J. G. Culotti, A. Coulson, D. G. Albertson, and M. Chalfie. mec-7 is a beta-tubulin gene required for the production of 15-prot filament microtubules in *Caenorhabditis elegans*. *Genes Dev.* 3:870–881, 1989.
- ³⁰Singh, A., S. Suri, T. Lee, J. M. Chilton, M. T. Cooke, W. Chen, J. Fu, S. L. Stice, H. Lu, T. C. McDevitt, and A. J. Garcia. Adhesion strength-based, label-free isolation of human pluripotent stem cells. *Nat. Methods* 10:438–444, 2013.
- ³¹Sokabe, M., F. Sachs, and Z. Q. Jing. Quantitative video microscopy of patch clamped membranes stress, strain, capacitance, and stretch channel activation. *Biophys. J.* 59:722–728, 1991.
- ³²Sukharev, S. I., P. Blount, B. Martinac, F. R. Blattner, and C. Kung. A large-conductance mechanosensitive channel in *E. coli* encoded by mscL alone. *Nature* 368:265–268, 1994.

- ³³Sukharev, S., S. R. Durell, and H. R. Guy. Structural models of the MscL gating mechanism. *Biophys. J.* 81:917–936, 2001.
- ³⁴Sukharev, S., and F. Sachs. Molecular force transduction by ion channels: diversity and unifying principles. *J. Cell Sci.* 125:3075–3083, 2012.
- ³⁵Sukharev, S. I., W. J. Sigurdson, C. Kung, and F. Sachs. Energetic and spatial parameters for gating of the bacterial large conductance mechanosensitive channel, MscL. *J. Gen. Physiol.* 113:525–540, 1999.
- ³⁶van den Bogaart, G., V. Krasnikov, and B. Poolman. Dual-color fluorescence-burst analysis to probe protein efflux through the mechanosensitive channel MscL. *Biophys. J.* 92:1233–1240, 2007.
- ³⁷Vogel, V., and M. P. Sheetz. Cell fate regulation by coupling mechanical cycles to biochemical signaling pathways. *Curr. Opin. Cell Biol.* 21:38–46, 2009.
- ³⁸White, C. R., and J. A. Frangos. The shear stress of it all: the cell membrane and mechanochemical transduction. *Philos. Trans. R. Soc. Lond. B Biol. Sci.* 362:1459–1467, 2007.
- ³⁹Xiong, W., N. Grillet, H. M. Elledge, T. F. Wagner, B. Zhao, K. R. Johnson, P. Kazmierczak, and U. Muller. TMHS is an integral component of the mechanotransduction machinery of cochlear hair cells. *Cell* 151:1283–1295, 2012.
- ⁴⁰Yoshimura, K., A. Batiza, M. Schroeder, P. Blount, and C. Kung. Hydrophilicity of a single residue within MscL correlates with increased channel mechanosensitivity. *Biophys. J.* 77:1960–1972, 1999.